Review Paper:

Effect of damage limit states on the seismic fragility of reinforced concrete frame-shear wall buildings

Mibang Durga* and Choudhury Satyabrata
Department of Civil Engineering, NIT Silchar, INDIA
*durgamibang28@gmail.com

Abstract

Assessment of the seismic vulnerability of frame-shear wall buildings can be performed by non-linear dynamic analysis and it needs detailed analytical modeling, structural performance measures and various earthquake intensities. The codal based design method can hardly be used for designing buildings of pre-defined target objectives whereas the Unified performance-based design (UPBD) method can be designed for buildings of pre-defined target objectives. In the current study, the UPBD method for frame-shear wall buildings has been applied for different performance levels (PL) i.e. Immediate occupancy (IO), Life safety (LS) and Collapse prevention (CP) with 1%, 2% and 3% drift in both the directions of the buildings.

The nonlinear dynamic analysis of the reinforced concrete (RC) frame-shear wall buildings is performed considering spectrum compatible ground motions (SCGM) as per EC-8 demand spectrum at 0.45g level and type B soil condition. Vulnerability assessment of the frame-shear wall buildings is conducted by generating fragility curves and the probability failure of structure is checked based on different configurations and damage limit states of the structure. Finally, the outcome of the work gives a proper idea of the nonlinear behavior of the dual system so that optimum design could be acquired for achieving higher safety aspects.

Keywords: Shear wall, UPBD Method, Peak inter-storey drift, Fragility.

Introduction

Buildings suffer damages under strong earthquake events. Reinforced concrete frame-shear wall buildings are popular building forms for medium to high rise buildings. Vulnerability assessment of such buildings in their inelastic range can be suitably performed through nonlinear dynamic analysis which necessitates detailed nonlinear modeling of the frame-shear wall buildings. Fragility analysis is the most important tool used for damage assessment of buildings[12,13,22,25]. Design codes are prescriptive in nature. Available literature has primarily focused on collapse damage states[1,8,11] of the structures in order to reduce seismic risk of the building during earthquakes.

Initially, the seismic fragility analysis was developed for nuclear plants[22] where fragility curves of various important equipment had been plotted. This method has been improved by Hwang et al[14] and it expanded its influences over the assessment on normal buildings. Many researchers conducted a dynamic analysis with different levels of buildings using different model types[18,19,23,26]. Fardis and Krawinkler[11] have worked on the assessment of the seismic performance of structures for both old and new shear wall buildings designed as per EC-8 and derived to see the performance of the structures through fragility curves.

Another study had been done by Pejovic and Jankovic[17] using Perform 3D software to find the assessment of the seismic vulnerability of tall RC buildings with core wall structural systems. Other recent works have focused on mid-rise frame-shear wall buildings conforming EC-8 for medium to high-class ductility[20] and on school buildings with the shear wall, for the loss assessment[6]. The hybrid approach has been used by Kappa et al[24] which consists of both experimental and analytical approaches. The shear wall can be modeled as a wide column plane shell or layered shell element. Nonlinear modeling and dynamic analysis of layered shear wall buildings using an approximate approach of seismic fragility analysis of buildings are scanty. Therefore, the present study primarily focuses on the modeling of shear walls with layered shell elements carrying out fragility analysis using an approximate approach.

The approximate method[2,21,31,32,36] is less time taking yet gives satisfactory results. UPBD method for RC frame building was presented by Choudhury and Singh[5] and this method accommodates both building drift and building PL (in context to the plastic rotation of members). It gives the member sizes at the beginning of the design thus avoiding iteration. Twelve numbers of RC frame-shear wall buildings with two different plans, four height categories and various target performance levels have been considered in the present study. The target design criteria considered are Immediate occupancy (IO) performance level (PL) with drift 1%, life safety PL with drift 2% and collapse prevention PL with drift of 3%.

The shear walls used in the finite element building have been modeled as layered shell elements. Buildings considered are 8-storey, 10-storey, 12-storey and 15-story. The design has been carried out considering EC-8[7] demand spectrum at 0.45g level and type B soil condition. The investigation involves non-linear dynamic analysis under 22 spectrum compatible ground motions (SCGM) which are generated using Seismo-match[28]. Various earthquake intensities are selected based on FEMA P-696[9] and the magnitudes of the earthquake data are in the range of 6.5 to 7.6. Seismic fragility analysis being one form of reliability analysis shows the exceedance probability (POE) of certain damage limit states for any given structures under seismic excitation for a particular intensity measure (IM).

The peak inter-story drift ratios (PIDR) are selected as the engineering demand parameter (EDP) to represent the global performance of considered buildings. Consecutively, the behavior of the building is identified based on a gradual increment of peak ground acceleration (PGA) and height of the buildings of different target performance objectives of the drifts and PL combinations considered as per FEMA-356 (Table 1-3)[10]. For generating seismic fragility curves at different intensity levels, an approximate approach of seismic fragility analysis has been used.

The major advantage behind selecting the approximate approach of seismic fragility analysis over the other available approaches is that it is computationally time-saving without the loss of accuracy in estimating the exceedance probability of damage limit state. In seismic fragility analysis, the PGA (g) has been considered as an IM and all the ground motion considered has been scaled to the expected level. The incorporation of scaled records captures the worst scenario of the structural degradation that could be identified. Finally, the output of the study will provide a better understanding of the building performance under seismic actions for various capacity limit states and configurations.

Design Philosophy of the buildings

Pettinga and Priestley[34] introduced a DDBD procedure for RC frame buildings. Sullivan et al developed the DDBD method for frame-shear wall buildings. In these two methods, only drift was considered as the target design criterion. But in the case of the UPBD method, it satisfied both drift and PL (in terms of plastic rotation of the members) and gave member sizes at the beginning of the design. No iteration is required for beam sizes, length and thickness of the walls. The beam sizes are obtained as per Choudhury and Singh[5].

Here, the multiple degrees of freedom (MDOF) system as displayed in fig. 1(a) are converted into an equivalent single degree of freedom (ESDOF) system as displayed in fig. 1(b). As per fig. 1, eq. (1) is obtained where, θ_d is the design drift which is the total summation of yield rotation (θ_{yw}) as well as plastic rotation of the wall (θ_{pw}).

$$\theta_d = \theta_{yw} + \theta_{pw} \qquad (1)$$

The yield rotation of the wall θ_{yw} and yield curvature ϕ_{yw} of wall[35] are given by eq. (2) and (3) respectively:

$$\theta_{yw} = \phi_{yw}\frac{h_{inf}}{2} \qquad (2)$$

$$\phi_{yw} = \frac{2\varepsilon_y}{L_w} \qquad (3)$$

where h_{inf} is inflection height of wall and ε_y is rebar yield strain of wall. Substituting eq. (2) and (3) in (1), eq. (4) is obtained:

$$L_w = \frac{\varepsilon_y h_{inf}}{\theta_d - \theta_{pw}} \qquad (4)$$

where L_w is the horizontal length of the wall. The beam depth satisfying the target criteria is given by eq. 5 by Choudhury and Singh[5]:

$$h_b = \frac{0.5\varepsilon_y l_b}{\theta_d - \theta_{pb}} \qquad (5)$$

In eq. 5, l_b is the length of the beam in the direction of seismic action, θ_{pb} is the allowable plastic rotation of beam for the PL considered. The beam width is considered as half to two-third of the depth of the beam as per common practice. Column size is found out by trial so that the column steel remains in the range of 3% to 4%. Alternatively, sizes of the column can be obtained as per Mayengbam and Choudhury[25]. The height of inflection (h_{inf}) is a parameter in frame-shear wall building design. The h_{inf} of frame shear wall can be determined by identifying the moments that are borne by the shear wall.

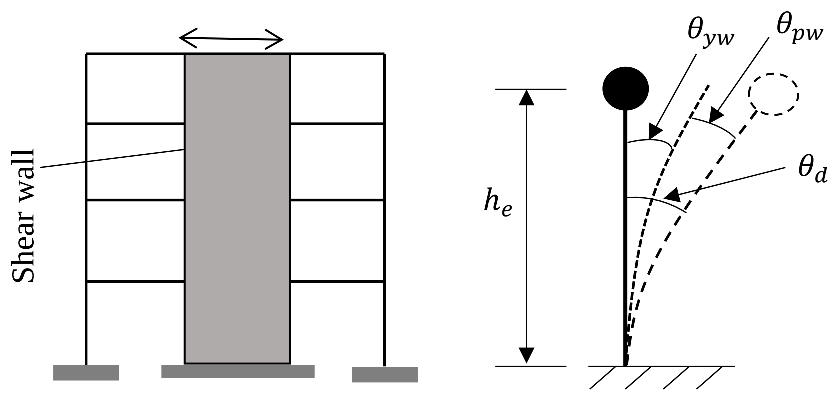

(a) MDOF system (b) ESDOF system

Figure 1: MDOF and ESDOF systems

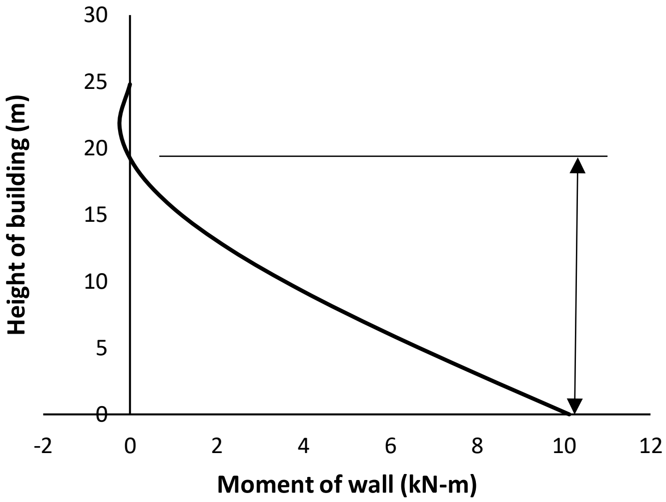

Figure 2: Inflection height of a typical building considered in the study.

Moments of the wall can be determined from the total moments from where the linear distribution of frame moments is subtracted. The detailed process can be seen in Priestley et al[34,35]. A typical drawing for inflection height is shown in fig. 2.

The MDOF building is converted to ESDOF system using equations 6 to 9:

$$\Delta_d = \frac{\sum_{i=1}^{N} m_i \Delta_i^2}{\sum_{i=1}^{n} m_i \Delta_i} \tag{6}$$

$$m_e = \frac{\sum_{i=1}^{N} m_i \Delta_i}{\Delta_d} \tag{7}$$

$$h_e = \frac{\sum_{i=1}^{N} m_i \Delta_i h_i}{\sum_{i=1}^{n} m_i \Delta_i} \tag{8}$$

$$\Delta_i = \Delta_{iyw} + \left(\theta_d - \phi_{yw} h_{inf}/2\right) h_i \tag{9}$$

where Δ_d is design displacement, m_e is effective mass, h_e is equivalent height, m_i is the mass of i^{th} storey, Δ_{iyw} is the yield displacements of the wall in i^{th} storey, h_i is the storey height of i^{th} floor from the base of the building, Δ_i is the profile displacement in the i^{th} floor and the number of stories in the building is denoted by N. The yield displacement profile of the wall is obtained using eq. 10:

$$\Delta_{iyw} = \frac{\emptyset_{yw} h_i h_{inf}}{2} - \frac{\emptyset_{yw} h_{inf}^2}{6}, \text{ when } h_i \geq h_{inf} \tag{10a}$$

$$\Delta_{iyw} = \frac{\emptyset_{yw} h_i^2}{2} - \frac{\emptyset_{yw} h_i^3}{6 h_{inf}}, \text{ when } h_i \leq h_{inf} \tag{10b}$$

$$\emptyset_{yw} = \frac{2\varepsilon_y}{L_w} \tag{10c}$$

Ductility demands of frames and walls[33] can be determined by using eq. 11 and eq. 12:

$$\mu_w = \frac{\Delta d}{\Delta_{he,y}} \tag{11}$$

$$\mu_f = \left(\frac{\Delta_i - \Delta_{i-1}}{h_i - h_{i-1}}\right) \frac{1}{\theta_{yf}} \tag{12}$$

where μ_w is the displacement ductility of the wall, yield displacement at the effective height level of wall is denoted by $\Delta_{he,y}$, Δ_{i-1} is the displacements at $(i-1)$-th floor, h_{i-1} is the height of $(i-1)^{th}$ floor, μ_f is the displacement ductility of the frame and, θ_{yf} is the frame yield drift. The equivalent damping of the ESDOF system is obtained from eq. 13 to 17:

$$\xi_{SDoF} = \frac{M_w \xi_w + M_{ot,f}\, \xi_f}{M_w + M_{ot,f}} \tag{13}$$

$$\xi_w = \frac{95}{1.3\pi}\left(1 - \mu_w^{-0.5} - 0.1 \times r \times \mu_w\right)\left(\frac{1}{(T_{e,trial}+0.85)^4}\right) \tag{14}$$

$$\xi_f = \frac{120}{1.3\pi}\left(1 - \mu_w^{-0.5} - 0.1 \times r \times \mu_f\right)\left(1 + \frac{1}{(T_{e,trial}+0.85)^4}\right) \tag{15}$$

$$T_{e,trial} = \frac{N}{6}\sqrt{\mu_{sys}} \tag{16}$$

$$\mu_{sys} = \frac{M_w \mu_w + M_{ot,f} \times \mu_f}{M_w + M_{ot,f}} \tag{17}$$

where M_w is wall moment, ξ_w is wall damping, $M_{ot,f}$ is frame overturning moment, ξ_f is frame damping, $T_{e,trial}$ is the trial effective time period, μ_{sys} is ESDOF system ductility and the post-yield stiffness ratio is denoted by r and 0.05 is generally considered for the new RC structures.

Displacement spectra corresponding to design spectra are drawn for various dampings. For this purpose, eq. 18 is utilized where η is the reduction factor corresponding to the damping. Displacement spectra corresponding to design spectra of EC-8 for soil type B and at 0.45g level are shown in fig. 3.

$$\eta = \sqrt{\frac{10}{(5+\xi_{ESDOF})}} \geq 0.55 \tag{18}$$

Effective stiffness K_e was found by the eq. 19 and the base shear V_b is expressed as per eq. 20:

$$K_e = \frac{4\pi^2 m_e}{T_e^2} \tag{19}$$

$$V_b = k_e \Delta_d \quad (20)$$

The computed base shear found by eq. 20 is distributed to different floors as per eq. 21:

$$F_i = \frac{m_i \Delta_i}{\sum_{i=1}^{n} m_i \Delta_i} V_b \quad (21)$$

where F_i is the force applied to different floors of the buildings.

The combinations of load used for design are:
$DL + LL$
$DL + LL \pm F_x$
$DL + LL \pm F_y$

where DL, LL, F_x, F_y stand for dead load, live load and earthquake load in x and y direction respectively. The design has been done using the expected strength of materials as per FEMA-365. Capacity design is done so that column to beam capacity ratio is more than 1.4 as per IS 13920[16].

Design of the representative buildings

12 numbers of frame-shear wall buildings have been considered for two different plans I and II. The height of buildings considered is 8, 10, 12 and 15 storeys. The plans and elevations of the considered buildings are shown in fig. 4.

The buildings have been designed using the UPBD method for target performance objectives of IO, LS and CP with 1% 2% and 3% drift. Consecutively, the structures have been designed with the expected strength as per FEMA-356 and the demand level of the EC-8 spectrum corresponding to the 0.45g hazard level. Finite element software SAP2000 v.21[29] has been used to model, design and analyze the buildings.

The characteristic strength of concrete is considered as 30 MPa and the yield strength of rebar is 500 MPa respectively. The floor height of buildings considered is kept constant to 3.1 m. Also, the column steel has been restricted to 3 - 4% of the cross-sectional area of the column.

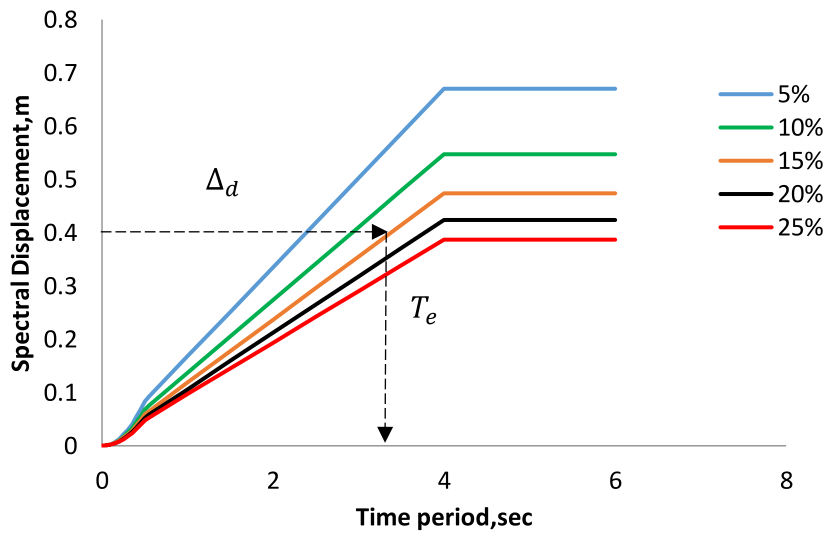

Figure 3: Displacement Spectra corresponding to design spectra of EC-8 for soil type B at 0.45g level.

Table 1
Nomenclature of the buildings considered and target design criteria

S.N.	Plan of the Building	Nomenclature of Buildings	Target performance level	Target drift %
1	I	B-8-IO	IO	1
2	I	B-10-IO		
3	I	B-12-IO		
4	I	B-15-IO		
5	I	B-8-LS	LS	2
6	II	B-10-LS		
7	II	B-12-LS		
8	II	B-15-LS		
9	II	B-8-CP	CP	3
10	II	B-10-CP		
11	II	B-12-CP		
12	II	B-15-CP		

Table 2
Dimensions related to the buildings considered

Building name	Column sizes (mm)		Beam size (mm)	Shear wall thickness (mm)	Length of wall (mm)
	Inner column	Outer column			
B-8-IO	800×800	900×900 850×850 800×800	1000×500	150	3000
B-10-IO	600×600	700×700 650×650 600×600	500×350	300	3500
B-12-IO	600×600	700×700 650×650 600×600	600×400	300	4000
B-15-IO	800×800	800×800 850×850 900×900	1000×500	300	5000
B-8-LS	700×700	800×800 750×750 700×700	700×450	150	5000
B-10-LS	550×550	650×650 600×600 550×550	700×400	300	6000
B-12-LS	650×650	750×750 700×700 650×650	900×450	300	7000
B-15-LS	700×700	800×800 750×750 730×730	600×350	300	8000
B-8-CP	600×600	700×700 650×650 600×600	500×350	150	7000
B-10-CP	600×600	700×700 650×650 600×600	500×350	200	8000
B-12-CP	600×600	700×700 650×650 600×600	650×450	200	10000
B-15-CP	730×730	780×780 750×750 730×730	750×500	300	12000

The nomenclature of the buildings has been listed in table 1. The buildings have been designated with 'B' and it has been contained within the nomenclature. The second term in the nomenclature represents the storey's height of the buildings and the last term signifies the performance level of the structure (IO, LS, or CP).

Further, the ultimate member's sizes of several buildings have been listed in table 2. The design is done in accordance with the expected strength specified by FEMA 356 with an expected concrete strength equal to 1.5 times the characteristics strength of concrete in 28 days and 1.25 times the yield strength of the rebar.

Nonlinear dynamic analysis

Several ground motion data are required for accurately performing the seismic fragility analysis. The present investigation involves 22 spectrum compatible ground motions (SCGM) that are generated using Seismo-Match details which are listed in table 3. The foremost benefit of using SCGM is that it makes the ground motion compatible with the design spectrum. The matched response spectra of the generated SCGMs for 22 ground motions with 5% damping with the design spectra of EC-8 are shown in fig. 7. In the current study, ground motions are scaled to a hazard level of 0.45g and applied in the short direction as well as the long direction of the buildings. The scaling of ground motions helps in finding the structural response up to the desired level of degradation of the structure. Therefore, with the incorporation of scaled records, the worst scenario of structural degradation could be identified.

Bommer et al[3] in their study found that SCGMs yield a comparatively lesser dispersion and such accelerograms can be used for computer-intensive NLTHA. Also, one of the major reasons for using such accelerograms is the non-availability of recorded ground motions in many seismic areas. The characteristics of the ground motions are represented in terms of intensity measure (IMs) which include PGA i.e. peak ground acceleration, SA i.e. spectral acceleration and PGV i.e. peak ground velocity. However, based on various studies conducted in recent years,[4,15,27] it has been found that PGA can be effectively used for reflecting the response of the structure under the probabilistic seismic framework. Henceforth, in the representative building, PGA is adopted for assessing the seismic fragility.

Seismic Fragility Analysis of Considered Buildings

Seismic fragility considering approximate approach: Seismic fragility is another form of reliability that expresses the probability of exceedance of a certain damage limit state for any given type of structure under seismic excitation. Several researches have been carried out in the past few decades that are associated with the seismic fragility of RC dual-frame buildings. However, there is no work done by designing the RC dual-frame building using UPBD Method. Fragility may be defined as the probability where the demand acting on the structure exceeds the capacity of the structure for a specified intensity measure (IM). Therefore, the expression of seismic fragility[30] can be expressed as eq. 22:

$$\text{Fragility} = \Pr[D \geq C/IM] = \Pr[C - D \leq 0.0/IM] \quad (22)$$

where D is the seismic demand, C is the capacity and IM is the ground motion intensity measure. Considering the time-variant effect on the seismic fragility of the RC frame-shear wall buildings, eq. 23 holds good[30]

$$\text{Fragility} = \Pr[D(t) \geq C(t)/IM = Pr[C(t) - D(t) \leq 0.0/IM] \quad (23)$$

Assuming that the seismic capacity and demand follow a lognormal distribution, eq. 23 takes the form of eq. 24:

$$\Pr[D(t) \geq \frac{C(t)}{IM} = \Phi\left[\frac{\ln\left(\frac{N_d(t)}{N_c(t)}\right)}{\sqrt{\beta^2_{D\backslash IM}(t)+\beta^2_C(t)}}\right] \quad (24)$$

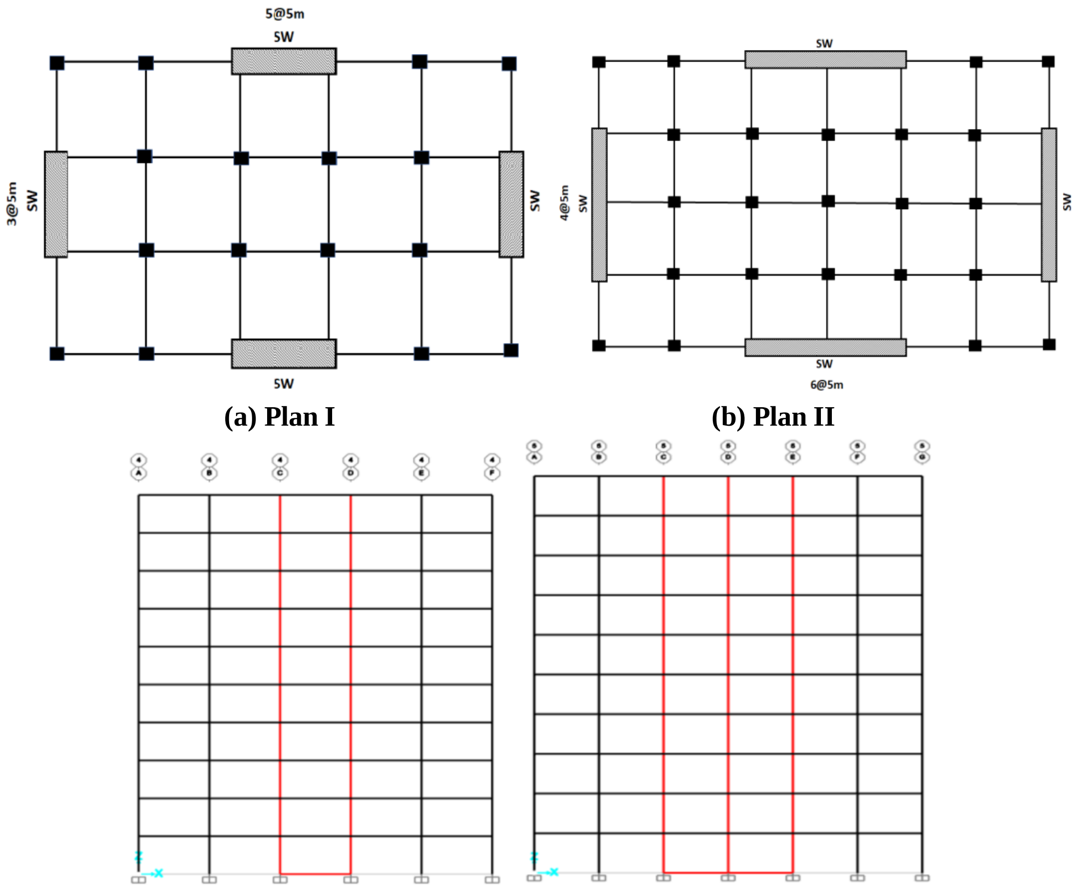

(a) Plan I

(b) Plan II

(c) Typical frame elevations

Figure 4: Building model considered in the study (a) Plan I (b) Plan II and (c) Typical elevations

Table 3
Artificial ground motion considered

S.N.	Name	Mw	Background Earthquake	Year of Occurrence
1	GM1	6.7	Northridge	1994
2	GM2	6.7	Northridge	1994
3	GM3	7.1	Duzce, Turkey	1999
4	GM4	7.1	Hector Mine	1999
5	GM5	6.5	Imperial Valley	1979
6	GM6	6.5	Imperial Valley	1979
7	GM7	6.9	Kobe, Japan	1995
8	GM8	6.9	Kobe, Japan	1995
9	GM9	7.5	Kocaeli, Turkey	1999
10	GM10	7.5	Kocaeli, Turkey	1999
11	GM11	7.3	Landers	1992
12	GM12	7.3	Landers	1992
13	GM13	6.9	Loma Prieta	1989
14	GM14	6.9	Loma Prieta	1989
15	GM15	7.4	Manjil, Iran	1990
16	GM16	6.5	Superstition Hills	1987
17	GM17	6.5	Superstition Hills	1987
18	GM18	7.0	Cape Mendocino	1992
19	GM19	7.6	Chi-Chi, Taiwan	1999
20	GM20	7.6	Chi-Chi, Taiwan	1999
21	GM21	6.6	San Fernando	1971
22	GM22	6.5	Friuli, Italy	1976

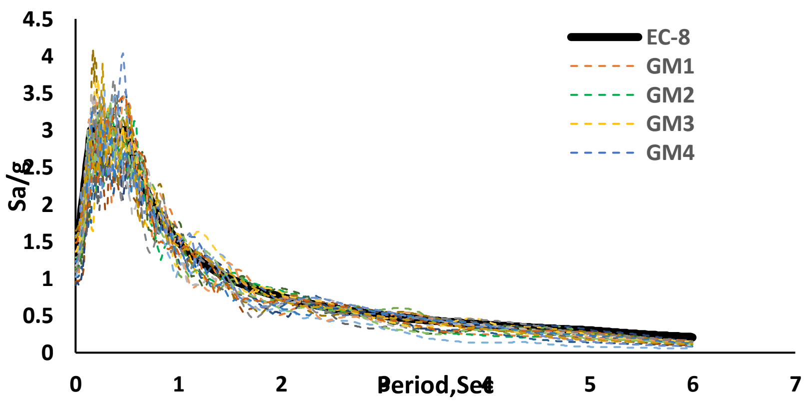

Figure 7: Matched response spectra of the generated SCGMs for 22 ground motions with 5% damping with the design spectrum of EC-8 (soil type B, at 0.45g level)

where $N_d(t)$ is the estimated median of the demand at the time t, $N_c(t)$ is the estimated median of the capacity at the time t, $\beta^2_{D\backslash IM}(t)$ is the dispersion of the demand at the time t and $\beta^2_{C\backslash IM}(t)$ is the dispersion of the capacity at the time t. The equation of the probabilistic seismic demand model (PSDM) is expressed in eq. 25:

$$\ln(N_d(t) = y(t) + z(t)\ln(IM) \quad (25)$$

Here, $y(t)$ and $z(t)$ are the parameters of regression that are estimated during the time t and it could be found by regressing the demands of buildings samples at different times.

Development of Fragility curves

A total of 12 finite elements (FE) models of the RC dual-frame buildings have been generated by applying the UPBD method. The generated building FE models are then paired with several selected ground motions considered and nonlinear dynamic analyses are carried out to obtain the structural response corresponding to each building model. The peak inter-story drift ratio (PIDR) is selected as an engineering demand parameter (EDP) to identify the overall performance of the building. Fragility analysis has been conducted for different PLs, namely IO, LS and CP as well as for different PGA values.

The PGA levels chosen here are 0.10g, 0.16g, 0.24g, 0.36g and 0.45g based on the vulnerability of the structure in various seismic zones across the globe. Further, PSDM at different PGA levels and storey heights has been generated based on eq. 25. Table 4 shows the generated probabilistic seismic demand models for different PGA levels and storey heights along with the statistical properties.

Results and Discussion

In this study, vulnerability assessment of the dual system is conducted by generating seismic fragility curves and the failure probability of the structure is checked based on different configurations and damage limit states of the structure. Here, the primary objective of the study is to focus on the seismic response of RC dual-frame buildings corresponding to drift demand (PIDR) that may be considered as one of the most detrimental forms of measures leading to failure of the structure under seismic excitation. The PIDR based probabilistic seismic demand model necessary for estimating the probability of exceedance (POE) for the considered damage limit states as given by eq. 26:

$$\ln(PGA) = a(t) + b(t)\ln(PIDR) \tag{26}$$

where $a(t)$ and $b(t)$ are the parameters of regression and peak inter-storey drift ratio (PIDR) obtained from the time history results. From the fragility curves, it has been observed that POE is higher under CP performance level as compared to other considered IO and LS performance levels as shown in fig. 8.

Also, it has been observed that in the case of 10- and 12-story buildings, the POE has negligible variation under IO and LS level; however, POE increases with heights of buildings under CP PL. Thus, the buildings under CP PL are highly susceptible to failure as compared to other buildings. Similarly, identical observations have been found in the second case of fragility analysis where the POE is estimated by varying the PGA capacities.

Fig. 9 shows exceedance probability with respect to variation in the PGA capacities. The PGA capacities, in this case, show a substantial increment in the POE, when the seismic capacity limit states have been reduced from 0.45g to 0.10g. Also, a higher POE is observed when the height of the building is gradually increased at the CP PL as compared to the other PLs. Specifically, the POE is maximum for a 15-storeys building under CP level.

Conclusion

In this study, the fragility of frame-shear wall buildings designed using the UPBD method has been presented. A total of 12 number of dual system buildings have been considered. The buildings considered included two plans and three height categories. The target performance criteria considered are IO, LS and CP with 1%, 2% and 3% drift. Layered shell element has been used in finite element modeling of shear walls. The novelty of the UPBD method used here is that it accommodates both drift and PL as design criteria. The member sizes are known at the beginning of the design without necessitating any iteration process. Displacement spectra corresponding to design spectra of EC-8 for B-type soil and seismicity level of 0.45g have been used. The designed buildings have been evaluated at the MCE level through nonlinear dynamic analyses 22 under SCGMs.

Table 4
Probabilistic seismic demand models for different PGA levels and storey heights along with the statistical properties

	Storey height (m)				**PL**	**R^2**	**Lognormal standard deviation**	**Lognormal mean**
	8th PSDMs	**10th PSDMs**	**12th PSDMs**	**15th PSDMs**				
0.1g	y=0.9573ln(x)-0.68	y=0.9573ln(x)-0.68	y=0.9843ln(x)-0.68	y=0.8637ln(x)-0.80	IO		0.90	-0.55
0.16g						0.95	0.89	-0.54
0.24g						0.95	0.93	-0.56
0.36g						0.98	0.93	-0.27
0.45g						0.86		
0.1g	y=0.9465ln(x)-1.53	y=0.9465ln(x)-1.53	y=0.913ln(x)-0.77	y=0.913ln(x)-0.77	LS	0.94	0.86	-0.55
0.16g						0.94	0.89	-0.52
0.24g						0.91	0.86	-0.40
0.36g						0.91	0.83	-0.01
0.45g								
0.1g	y=0.913ln(x)-0.77	y=0.913ln(x)-0.77		y=0.9573ln(x)-1.85	CP		0.86	0.45
0.16g						0.91	0.86	0.47
0.24g			y=0.9869ln(x)-1.84			0.91	0.92	-0.54
0.36g						0.98	0.93	-0.55
0.45g						0.95		

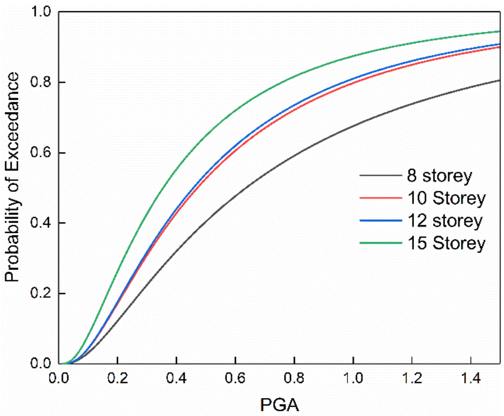

Figure 8(a) : IO Performance level

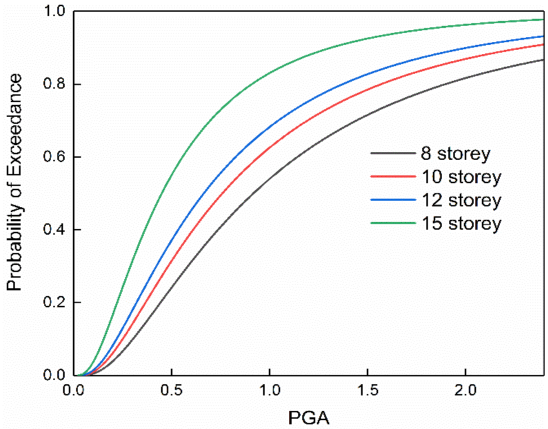

Figure 8(b) : LS Performance level

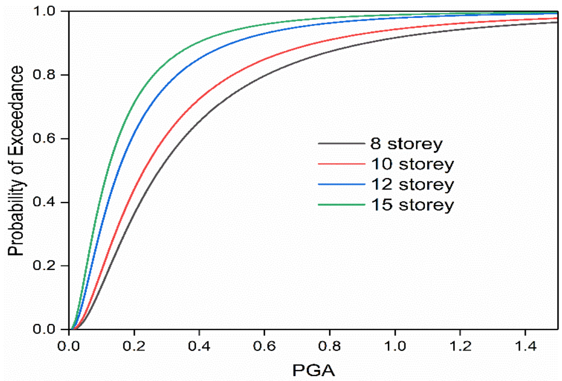

Figure 8(c): CP Performance level

Figure 8: Fragility curve with respect to storey (a) IO Performance level (b) LS Performance level (c) CP Performance level

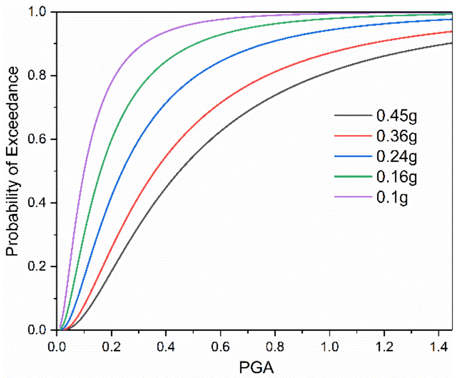

B-8-IO (long direction)

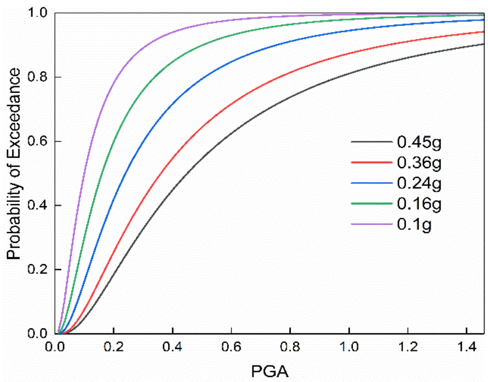

B-8-IO (short direction)

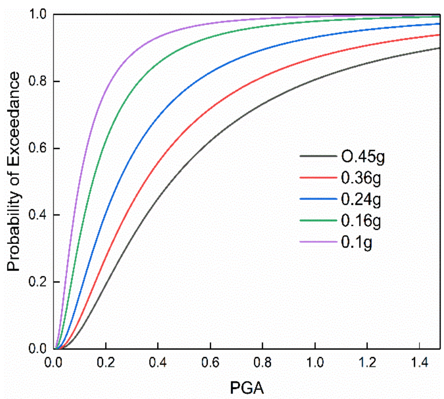

B-12-IO (long direction)

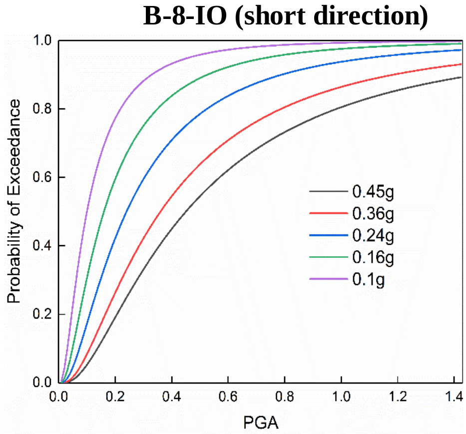

B-12-IO (short direction)

Figure 9 (a): Fragility curve of typical buildings with respect to PGA of 8,10 and 12 IO level Performance level

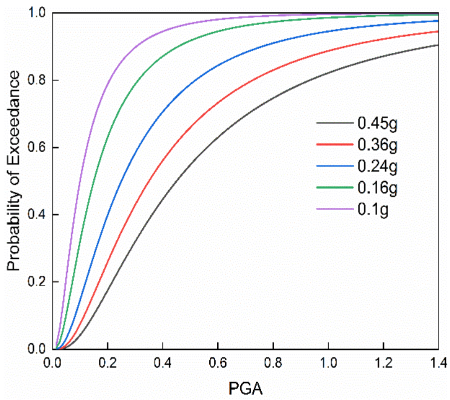

B-8-LS (long direction)

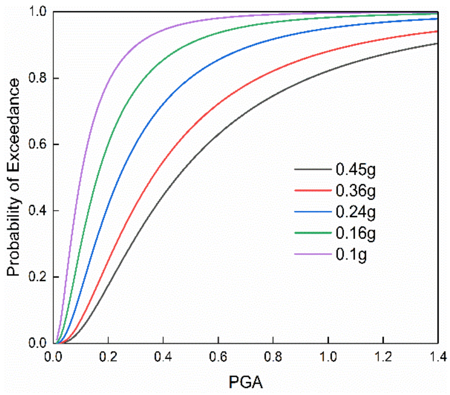

B-8-LS (short direction)

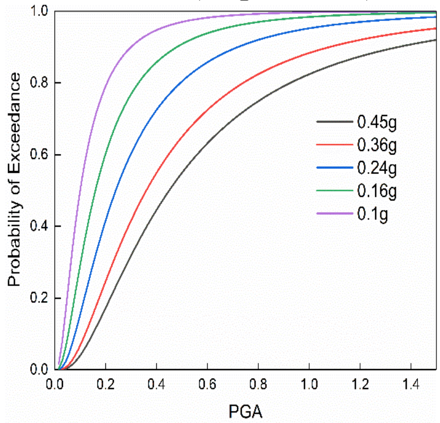

B-12-LS (long direction)

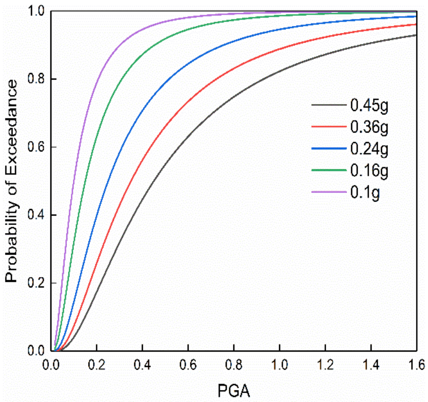

B-12-LS (short direction)

Figure 9 (b): Fragility curve of typical buildings with respect to PGA of 8 and 12 LS level (long direction) Performance level

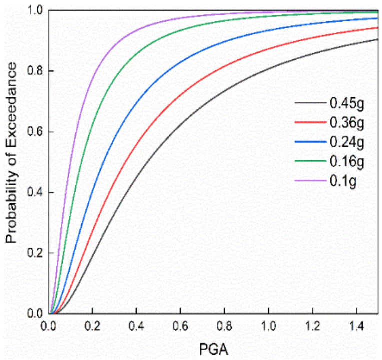

B-8-CP (long direction)

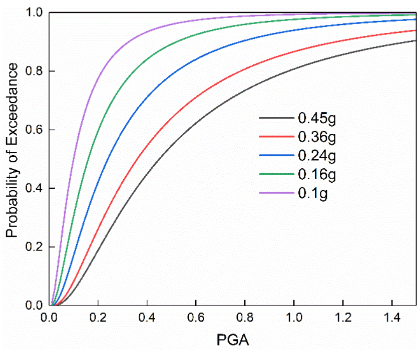

B-8-CP (short direction)

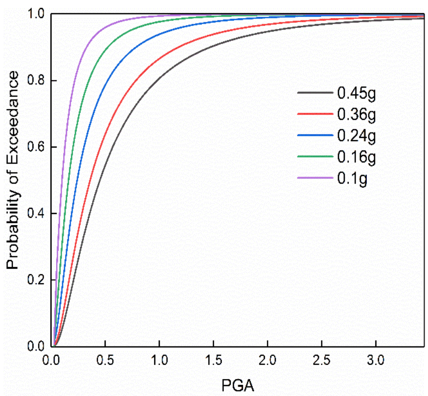

B-12-CP (long direction)

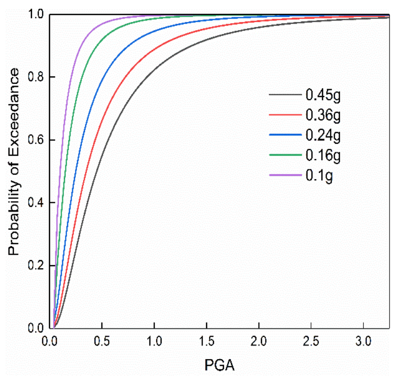

B-12-CP (short direction)

Figure 9 (c): Fragility curve of typical buildings with respect to PGA of 8 and 12 CP level (long direction) Performance level.

The POE has been estimated at different performance levels. For performing seismic fragility analysis, approximate approach has been used. The benefit of implementing an approximate approach over the other available approaches of seismic fragility analysis is that it is efficient in accurately estimating the exceedance probability of the damage limit states without tedious computational requirements. Peak inter-storey drift ratio (PIDR) has been taken engineering demand parameter (EDP). The outcome of the study put forwards a clear picture of the nonlinear behavior of shear wall buildings depicting the increment of POE with respect to geometry as well as site conditions (that is, site-specific PGA values) such that proper decision could be made for optimum design of the buildings which will eventually lead to higher safety.

Future work in this domain may involve the effect of multiple demand parameters on the exceedance probability of RC dual systems designed using the UPBD method. The work will help in capturing a broader picture of the nonlinear behavior of a dual system when multiple degradation parameters such as PIDR, joint rotation, displacement, column curvature etc. are combinely considered for generating the PSDM.

References

1. Attar S. and Liel A.B., Seismic performance of nonductile reinforced concrete frames with masonry infill walls-II: collapse assessment, *Earthquake Spectra*, **32**, 819-842 **(2016)**

2. Borele S.V. and Datta D., Damage assessment of structural system using fragility curves, *Journal Civil Engineering and Environment Technology*, **2(11),** 72-76 **(2015)**

3. Bommer Julian J. Acevedo and Beatriz, The use of real earthquake accelerograms as input to dynamic analysis, *Journal of Earthquake Engineering*, **8(1),** 43-91 **(2004)**

4. Gencturk B., Elnashai A.S. and Song J., Improved fragility relationships for populations of buildings based on the inelastic response, 14th world conference on earthquake engineering, 12-17 **(2008)**

5. Choudhury S. and Singh S.M., A Unified Approach to Performance-Based Design of RC Frame Buildings, *Journal of the Institution of Engineers (India) Series A*, **94(2),** 73-82 **(2013)**

6. Michel C., Hannewald P., Lestuzzi P., Fah D. and Husen S., Probabilistic mechanics-based loss scenarios for school buildings in Basel (Switzerland), *Bulletin of Earthquake Engineering*, **17(4)**, 1-26 **(2016)**

7. Eurocode 8, Design of Structures for Earthquake Resistance, Part 1: General Rules, Seismic Actions and Rules for Buildings Comite European de Normalization, Brussels **(2004)**

8. Elkady A. and Lignos D.G., Modeling of the composite action in fully restrained beam-to-column connections: implications in the seismic design and collapse capacity of steel special moment frames, *Earthquake Engineering and Structural Dynamics*, **43**, 1935-1954 **(2014)**

9. FEMA P-695, Methodology for Quantification of Building Seismic Performance Factors, NEHRP Consultants Joint Venture A partnership of the Applied Technology Council and the Consortium of Universities for Research in Earthquake Engineering **(2010)**

10. FEMA 356 Prestandard and commentary for the seismic rehabilitation of the building, Rehabilitation **(2000)**

11. Zareian F. and Krawinkler H., Structural system parameter selection based on collapse potential of buildings in earthquakes, *Journal of Structural Engineering*, **136**, 933-943 **(2010)**

12. Galanis P.H. and Moehle J.P., Development of collapse indicators for risk assessment of older-type reinforced concrete buildings, *Earthquake Spectra*, **31**, 1991-2006 **(2015)**

13. Gogus A. and Wallace J.W., Seismic safety evaluation of reinforced concrete walls through FEMA P695 methodology, *Journal of Structural Engineering*, **141(10)**, 141 **(2015)**

14. Hwang B.H.H.M. and Jaw J., Probabilistic damage analysis of structures, *Journal of Structural Engineering*, **116(7)**, 1992-2007 **(1990)**

15. Huanjun Jiang, Xiaojuan Liu and Lingling Hu, Seismic Fragility Assessment of RC Frame-Shear Wall Structures Designed According to the Current Chinese Seismic Design Code, *Journal of Asian Architecture and Building Engineering*, **14(2),** 459-466 **(2015)**

16. IS 13920, Ductile design and detailing of the reinforced concrete structure subjected to seismic force, Bureau of Indian Standards, New Delhi, India **(2016)**

17. Pejovic J. and Jankovic S., Seismic fragility assessment for reinforced concrete high-rise buildings in Southern Euro-Mediterranean zone, *Bulletin of Earthquake Engineering*, **14(1)**, 1-28 **(2015)**

18. Ji J., Elnashai A.S. and Kuchma D.A., An analytical framework for seismic fragility analysis of RC high-rise buildings, *Engineering Structures*, **29**, 3197-3209 **(2007)**

19. Ji J., Elnashai A.S. and Kuchma D.A., Seismic fragility relationships of reinforced concrete high-rise buildings, *Structural Design of Tall and Special Buildings*, **18**, 259-277 **(2009)**

20. Antoniou K., Tsionis G. and Fardis M.N., Inelastic shears in ductile RC walls of mid-rise wall-frame buildings and comparison to Eurocode 8, *Bulletin of Earthquake Engineering*, **13**, 841-869 **(2015)**

21. Korkmaz K., Evaluation of seismic fragility analyses, In The 14th world conference on earthquake engineering **(2008)**

22. Kennedy R.P. and Ravindra M.K., Seismic fragilities for nuclear power plant risk studies, *Nuclear Engineering and Design*, **79(1)**, 47-68 **(1984)**

23. Kolozvari K., Terzic V. and Saldana D., Implications of modeling assumptions on the loss estimation for shear wall buildings, in Proceedings of Structures Conferences, 6-8 **(2017)**

24. Kappos A.J., Panagopoulos G., Panagiotopoulos C. and Penelis G., A hybrid method for the vulnerability assessment of RC and URM buildings, *Bulletin of Earthquake Engineering*, **4(4),** 391-413 **(2006)**

25. Mayengbam S. and Choudhury S., Determination of column size for the displacement-based design of reinforced concrete frame buildings, *Journal of Earthquake Engineering and Structural Dynamics*, **43(8),** 1149-1172 **(2014)**

26. Nazari Y.R. and Saatcioglu M., Seismic vulnerability assessment of concrete shear wall buildings through fragility analysis, *Journal of Building Engineering*, **12**, 202-209 **(2017)**

27. Panpan Zhai, Peng Zhao, Yang Lu, Chenying Ye and Feng Xiong, Seismic Fragility Analysis of Buildings Based on Double-Parameter Damage Models considering Soil-Structure Interaction, *Advances in Materials Science and Engineering*, DOI:10.1155/2019/4592847, 13 **(2019)**

28. Seismomatch, Software Generation of spectrum compatible ground motion **(2016)**

29. SAP2000, v.21 Structural analysis programme, Berkley, CA, USA: Computer and Structures Inc.

30. Sudret B. and Mai C.V., Computing seismic fragility curves using polynomial chaos expansions, 11th International conference on structural safety and reliability **(2013)**

31. Sil A. and Longmailai T., Drift reliability assessment of a four-storey residential building under seismic loading considering multiple factors, *Journals of the Institutions of Engineers,* **98(3)**, 245-256 **(2017)**

32. Sil A., Gourab D. and Pritam H., Characteristics of FBD and DDBD techniques for SMRF buildings designed for seismic zone-V in India, *Journal Build Pathology Rehabilitation,* **14(1)**, 10-18 **(2019)**

33. Sullivan T.J., Priestley M.J.N. and Calvi G.M., Direct Displacement-Based Design of Frame-Wall Structures, *Journal of Earthquake Engineering,* **10(Special Issue 1),** 91-124 **(2006)**

34. Priestley M.J.N., Grant D.N. and Blandon Carlos A., Direct Displacement - based seismic design, Pavia, Italy **(2005)**

35. Priestley M.J.N., Calvi G.M. and Kowalaski M.J., Displacement based seismic design of structures, Pavia, Italy **(2007)**

36. Reveillere A., Gehl P., Seyedi D. and Modaressi H., Development of seismic fragility curves for damaged reinforced concrete structures, 15th world conference on earthquake Engineering **(2012)**.

(Received 13th April 2021, accepted 18th June 2021)

*****